Eur J Nucl Med Mol Imaging (2013) 40:565–573
DOI 10.1007/s00259-012-2304-8

ORIGINAL ARTICLE

Automatic semi-quantification of [^{123}I]FP-CIT SPECT scans in healthy volunteers using BasGan version 2: results from the ENC-DAT database

Flavio Nobili · Mehrdad Naseri · Fabrizio De Carli · Susan Asenbaum · Jan Booij · Jacques Darcourt · Peter Ell · Özlem Kapucu · Paul Kemp · Claus Varer · Silvia Morbelli · Marco Pagani · Osama Sabri · Klaus Tatsch · Livia Tossici-Bolt · Terez Sera · Tierry Vander Borght · Koen Van Laere · Andrea Varrone

Received: 21 August 2012 / Accepted: 9 November 2012 / Published online: 12 December 2012

Abstract
Purpose The aim of this study was to assess striatal dopamine transporter (DAT) availability in a large group of normal subjects.
Methods The study included 122 healthy subjects, aged 18–83 years, recruited in the multicentre 'ENC-DAT' study (promoted by the European Association of Nuclear Medicine). Brain single photon emission computed tomography (SPECT) was acquired by means of dual-head cameras 3 h after [^{123}I]FP-CIT administration. Specific to nondisplaceable binding ratios (SBRs) in the basal ganglia were computed using the 'BasGan' software, allowing automatic

F. Nobili (✉)
Clinical Neurophysiology, Department of Neurosciences, Ophthalmology and Genetics, University of Genoa, Genoa, Italy
e-mail: flaviomariano.nobili@hsanmartino.liguria.it

M. Naseri · S. Morbelli
Nuclear Medicine Unit, Department of Internal Medicine, University of Genoa, Genoa, Italy

F. De Carli
Institute of Bioimaging and Molecular Physiology, National Research Council, Genoa, Italy

S. Asenbaum
Department of Neurology, Medical University of Vienna, Vienna, Austria

J. Booij
Department of Nuclear Medicine, Academic Medical Center, University of Amsterdam, Amsterdam, The Netherlands

J. Darcourt
Nuclear Medicine Department Centre Antoine Lacassagne TIRO Laboratory CEA, University of Nice Sophia Antipolis, Nice, France

P. Ell
Institute of Nuclear Medicine, University College London Hospitals NHS Trust, London, UK

Ö. Kapucu
Department of Nuclear Medicine, Gazi Hospital, Gazi University School of Medicine, Besevler, Ankara, Turkey

P. Kemp
Department of Nuclear Medicine, Southampton University Hospitals Trust, Southampton, UK

C. Varer
Neurobiology Research Unit and Center for Integrated Molecular Brain Imaging (CIMBI), Copenhagen University Hospital, Rigshospitalet, Copenhagen, Denmark

M. Pagani
Department of Nuclear Medicine, Karolinska University Hospital, Stockholm, Sweden

M. Pagani
Institute of Cognitive Sciences and Technologies, Consiglio Nazionale delle Ricerche (CNR), Rome, Italy

O. Sabri
Department of Nuclear Medicine, University of Leipzig, Leipzig, Germany

K. Tatsch
Department of Nuclear Medicine, Municipal Hospital of Karlsruhe Inc., Karlsruhe, Germany

L. Tossici-Bolt
Department of Medical Physics and Bioengineering, Southampton University Hospitals NHS Trust, Tremona Road, Southampton SO16 6YD, UK

T. Sera
Department of Nuclear Medicine and Euromedic Szeged, University of Szeged, Szeged, Hungary

value extraction with partial volume effect correction. Multicentre camera inhomogeneity was taken into account by calibrating values on basal ganglia phantom data. SBR in each caudate nucleus (C) and putamen (P) were the dependent variables in a repeated measures general linear model analysis; age, gender, handedness and body mass index (BMI) were the independent variables.

Results SBR values in C and P were significantly associated with age (mean rate decrease with age: 0.0306 per year, or 0.57 % of the general mean; $p<0.0001$) and gender (women had higher values; $p=0.015$), while no significant effect was found for handedness and BMI. A significant interaction was found between age and region ($p<0.0001$) as the age-related decline was 0.028 for left C, 0.026 for right C and 0.034 for both P. P/C ratio analysis confirmed that age-related SBR decrease was stronger in P than in C ($p<0.0001$). No significant effect was found for season or time of the day when the scan was acquired by analysing the residual of SBR values in C and P, after subtraction of age and gender effects.

Conclusion This study confirms the dependency of DAT on ageing and highlights the gender differences in a large sample of healthy subjects, while it does not support the dependency of DAT on BMI, handedness, circadian rhythm or season.

Keywords [^{123}I]FP-CIT · DAT · Brain SPECT · Basal ganglia · BasGan software · Healthy subjects

Introduction

Single photon emission computed tomography (SPECT) imaging of the dopamine transporter (DAT) is widely used to assess the nigrostriatal function in parkinsonian syndromes. At the moment, [^{123}I]FP-CIT (^{123}I-ioflupane, DaTSCAN®, GE Healthcare) is by far the most widely used radiotracer, at least in Europe. In routine clinical studies, the majority of diagnostic scans can be easily reported by simple visual analysis by an expert reader. Also, a categorization of visual analysis has been successfully applied in research work [1]. In a study comparing this visual scoring system with a region of interest (ROI) method, there was no significant difference in sensitivity and specificity to detect loss of striatal DAT in Parkinson's disease (PD), PD dementia and dementia with Lewy bodies versus either controls or patients with Alzheimer's disease (AD). However, the positive predictive value and the likelihood ratio were definitely better with the ROI method in the differentiation between patients with these parkinsonisms and the group with AD, despite the fact that the ROI method was not anatomically based [2].

Moreover, semi-quantification of striatal DAT binding appears to be a valuable tool to generate numerical values to correlate with other disease markers, such as those expressing the severity of motor impairment, to assess the progression of diseases [3] and to monitor the effects of neuroprotective agents [4]. Another issue is the inter-rater reproducibility of qualitative analysis that may be low in 'borderline' scans in which subtle deficits may be reported or not.

Thus, the need for semi-quantification derived by means of automatic, unsupervised tools has grown in recent years and several methods have been proposed [5–11]. By means of these methods, three-dimensional (3-D) semi-quantification of striatal tracer binding has been achieved. Advantages over non-anatomic ROI methods include a lower inter- and intra-observer variability, the inclusion of the whole volume of the striatum and the possibility to longitudinally follow alterations in an individual patient. Finally, multicentre studies are feasible only if a shared semi-quantification method is adopted.

In this large, multicentre European study promoted by the Neuroimaging Committee (ENC-DAT) of the European Association of Nuclear Medicine (EANM) we applied the automatic, 3-D ROI semi-quantification software named 'BasGan' [12] to obtain DAT binding values from 122 healthy subjects studied with a dual-head gamma camera, the most widely distributed SPECT device in Europe. The effect of age, gender, body mass index (BMI), handedness, time and season of examination on DAT uptake was explored.

Materials and methods

Subjects

A total of 151 healthy controls (80 men, 71 women, age 20–83 years, mean 53) were included in the study by 13 centres in 10 European countries. The health status of subjects was carefully checked by means of medical history, blood chemistry, general medical and neurological evaluation, including the Unified Parkinson's Disease Rating Scale (UPDRS), and psychiatric evaluation, including the symptom checklist (SCL)-90-R [13] and the Beck Depression Inventory (BDI) [14] scales. General cognition was assessed by means

T. V. Borght
Nuclear Medicine Division, Mont-Godinne Medical Center, Université Catholique de Louvain, Yvoir, Belgium

K. Van Laere
Division of Nuclear Medicine, University Hospitals Leuven, Leuven, Belgium

A. Varrone
Centre for Psychiatry Research, Karolinska Institutet, Karolinska Hospital, Stockholm, Sweden

of the Mini-Mental State Examination (MMSE). Handedness was assessed with the Edinburgh Inventory. All subjects underwent structural volumetric MRI according to the imaging protocol of the recruiting centre.

Inclusion criteria were (1) UPDRS-III score=0 in subjects younger than 60 or <5 in older subjects; (2) Global Score Index <64 on the SCL-90-R; (3) score <10 on the BDI; (4) score >27 on the MMSE; and (5) a fully normal MRI in subjects younger than 60; however, white matter hyperintensities in T2-weighted images, corresponding to a white matter lesion (WML) score <3 on the Fazekas scale [15], were accepted in older subjects, provided that the basal ganglia were spared.

A history of parkinsonism in first-degree relatives and a positive urine test for pregnancy or recreational drug use on the day of SPECT examination were exclusion criteria.

The protocol was submitted and approved by the Ethics Committee in each of the 13 centres; informed consent was signed by all participants.

SPECT imaging and semi-quantification

Before a centre was qualified to participate in the ENC-DAT study and during the study period, a rigorous quality control protocol was applied for site certification. Moreover, SPECT images from an anthropomorphic striatal phantom (Radiology Support Devices Inc., Long Beach, CA, USA) filled with different concentrations of ^{123}I were acquired in all centres on a number of imaging systems with parallel collimation (see [16, 17] for further technical details). The protocol for filling of the phantom has been reported previously [17]. The purpose of the phantom study was to assess the different imaging systems for both their SPECT uniformity and the linearity of their response to ^{123}I.

[^{123}I]FP-CIT (DaTSCAN®) was injected intravenously at a dose of approximately 185 MBq, preceded by thyroid blockade according to the local procedure. Scans were obtained at 3 h and also at 4 h (optional) after tracer injection.

The present report deals with scans at 3 h and with those acquired on a dual-head camera system, using parallel-hole, low-energy high-resolution (LEHR) or low-energy ultrahigh-resolution (LEUHR) collimators, the most widely distributed SPECT system in Europe. The data of 122 subjects were included in the final analysis. Adding the other 29 subjects in whom imaging data were acquired with fan-beam collimators, triple-head camera or dedicated brain camera systems might have increased data inhomogeneity without adding a corresponding advantage in terms of number of subjects. Moreover, data analysis focused on scans corrected for attenuation but uncorrected for scatter and septal penetration, which is again the default mode of acquisition in most European centres. By adopting these choices, we aimed at reproducing the real world of [^{123}I]FP-CIT SPECT.

The acquisition parameters were as follows: rotational radius between 13 and 15 cm with appropriate patient safeguard, matrix 128×128, angular sampling ≤ 3° (360° rotation) and hardware zoom (1.23–2) to achieve a pixel size of 2–3 mm. The total scan time which was dependent on system type was determined as the time by which 2 million photopeak (159 keV ±10 %; 143–175 keV) counts were detected. Typically this ranged between 30 and 45 min.

Raw SPECT projection data in DICOM or interfile format were analysed by a centre core lab in Southampton. Reconstruction was performed using the ordered subset expectation maximization (OSEM) algorithm, with 10 iterations and 10 subsets for sets of 120 projections, and with 12 iterations and 8 subsets for sets of 128 projections to maintain an equivalent number of total EM iterations [16]. A 3-D post-filtering was applied to the reconstructed slices, using a Butterworth filter (defined as $1/B = \sqrt{1 + (f/f_c)^{2n}}$ with f_c = cut-off frequency and n = order), with cut-off = 0.50 cm^{-1} as defined on Link workstations, (1.2 cm^{-1} cut-off as defined on Hermes) and order 10.

OSEM reconstructions were performed also including calculated attenuation correction. The beam attenuation coefficient for 159 keV gamma rays in water was set to μ= 0.11 cm^{-1} [16].

Reconstructed images were sent by the core lab to Genoa for semi-quantification through the BasGan V2 software, allowing automatic, 3-D segmentation of caudate and putamen in each hemisphere. BasGan [12] is based on a high-definition, 3-D striatal template, derived from Talairach's atlas. An optimization protocol automatically performs fine adjustments in the positioning of blurred templates to best match the radioactive counts and locates occipital ROI for background evaluation. Partial volume effect (PVE) correction is included in the process of binding computation of the caudate nucleus, putamen and background (in occipital cortex). The PVE correction performed by the method (detailed in [12]) consists in an activity assignment in a Talairach-Tournoux atlas-based three-compartment model of basal ganglia. Putamen and caudate nucleus binding was subtracted by background binding as follows [(caudate nucleus or putamen binding−background binding)/background binding] to derive as outcome measure the specific to nondisplaceable binding ratio (SBR) in the caudate nucleus and the putamen in each hemisphere. Version 2 of the BasGan software (BasGan V2), freely available on the website of the Italian Association of Nuclear Medicine (http://www.aimn.it/struttura/gruppi/gs_neuro.php), was applied to images of the 122 subjects as well as to images of phantom acquisitions coming from each centre in order to calibrate results according to the phantom data.

From the four calibrated values, the ratio between SBR in putamen and in caudate nucleus was computed in each hemisphere (P/C ratio). Finally, asymmetries between SBR in caudate as well as in putamen were computed as follows:

Table 1 Mean (±SD) SBR values of DAT in caudate and putamen in each hemisphere in the whole subject sample, as well as in woman and in man subgroups

	No.	Mean	SD	Minimum	Maximum
All subjects					
Left caudate	122	5.538	1.101	2.773	8.517
Right caudate	122	5.658	1.098	3.108	8.305
Left putamen	122	5.152	1.096	2.627	8.270
Right putamen	122	5.153	1.111	2.811	8.393
P/C ratio (mean of two sides)	122	0.920	0.062	0.767	1.065
Men					
Left caudate	67	5.351	1.036	2.920	7.232
Right caudate	67	5.437	1.017	3.108	7.769
Left putamen	67	4.956	1.016	2.627	7.366
Right putamen	67	4.954	1.034	2.811	7.768
P/C ratio (mean of two sides)	67	0.920	0.066	0.767	1.065
Women					
Left caudate	55	5.767	1.144	2.773	8.517
Right caudate	55	5.923	1.140	3.213	8.305
Left putamen	55	5.392	1.151	2.627	8.270
Right putamen	55	5.396	1.161	3.067	8.393
P/C ratio (mean of two sides)	55	0.922	0.059	0.800	1.045

$$\mathrm{C(or\ P)percent\ asymmetry} = \left[(\mathrm{leftC} - \mathrm{rightC}) \Big/ \frac{1}{2}(\mathrm{leftC} + \mathrm{rightC})\right] * 100$$

Thus, a positive asymmetry stands for higher values in the left hemisphere and negative asymmetry for higher values in the right hemisphere. Finally, asymmetries were also considered as absolute values, i.e. independently of the sign.

Statistics

SBR in each caudate nucleus and putamen were the dependent variables in a repeated measures general linear model (GLM) analysis. The independent variables were (1) age, (2) gender, (3) handedness and (4) BMI. As far as significant effects were found, post hoc analysis was performed to evaluate differences between levels of factors. As for differences between regions (i.e. putamen and caudate nucleus in each hemisphere), post hoc investigation included the analysis of P/C ratio and asymmetries. Possible effects of season and time of day when the scan was acquired were evaluated in a subsequent analysis by means of repeated measures analysis of variance, in which the dependent variables were the residuals of SBR in each caudate nucleus and putamen, after the application of the previous GLM, and the independent factors were the season (four levels) and the time of day (classified into three levels: before 11 a.m., between 11 and 1 p.m. and after 1 p.m.). The distributions of SBR in each caudate nucleus and putamen around relevant mean values were checked for

Table 2 Results of repeated measures analysis of variance by GLM of 122 DAT SPECT in healthy volunteers. The dependent variable is SBR in four regions: left and right caudate and putamen. The effects of handedness and BMI as well as their interactions were excluded in a first step as they were by no means significant

	Degrees of freedom	Mean square	*F*	*p*
Between-subject effects				
Gender	1	15.56	4.77	0.0309
Age	1	151.34	46.41	0.0000
Gender * age	1	6.58	2.02	NS
Error	118	3.26		
Within-subject effects				
Region	3	0.054	0.79	NS
Region * gender	3	0.093	1.36	NS
Region * age	3	0.56	8.17	0.0000
Region * gender * age	3	0.069	1.00	NS
Error	354	0.069		

normality by the Shapiro-Wilk W test applied to the residuals after GLM.

On the basis of GLM analysis, formulas were provided to enable the estimation of expected SBR values and relevant prediction intervals, that is the intervals in which a single measure from a healthy subject is expected to be included with a 95 % probability.

Statistical analysis was performed by the Statistica software (StatSoft Inc.) [18]. All effects with significance level less than 0.05 were examined.

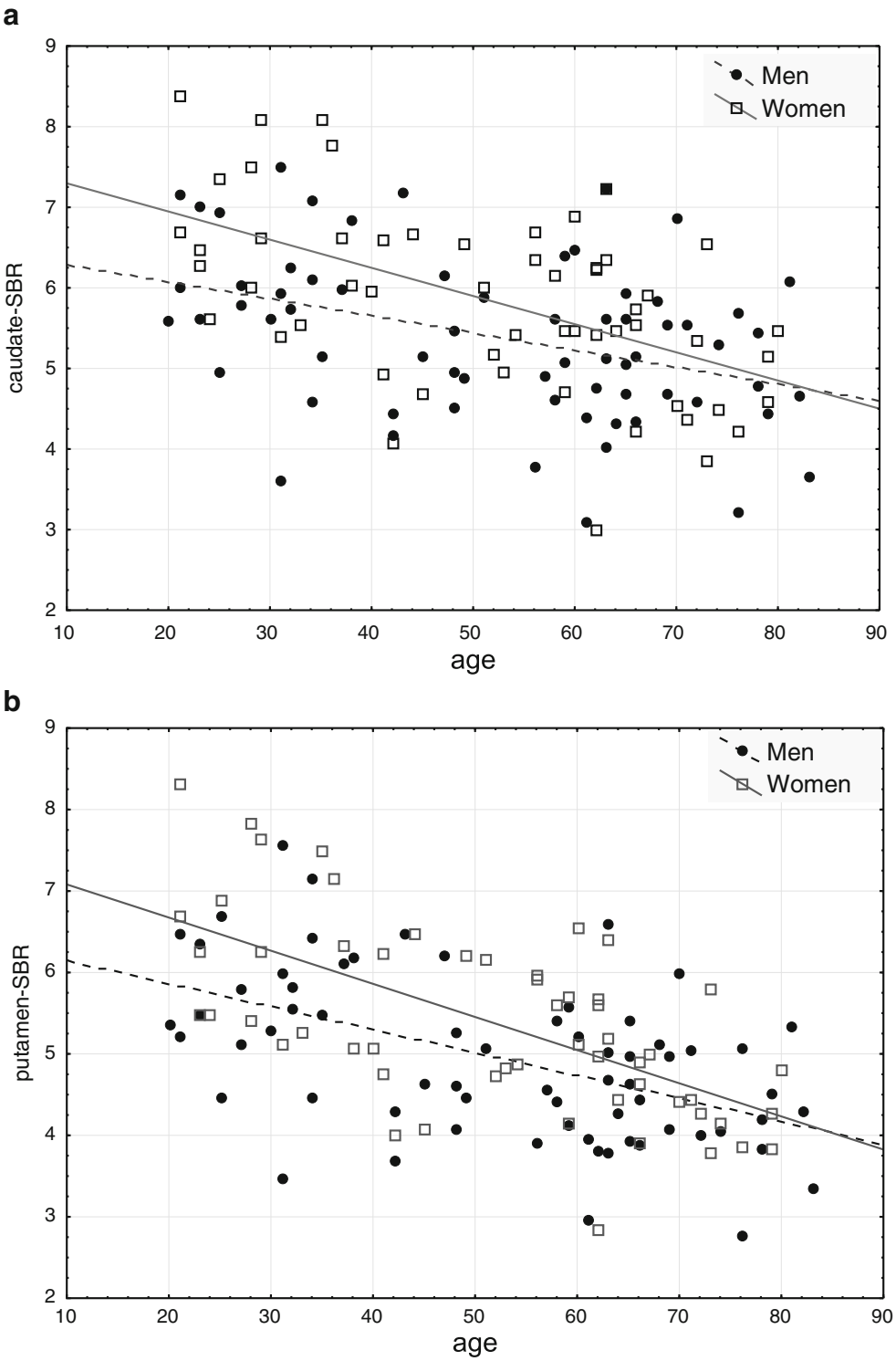

Fig. 1 Scatter plot of SBR as a function of age in caudate nucleus (**a**) and putamen (**b**). Data relevant to men (*closed circles*) and women (*empty squares*) have been independently fitted by linear regression lines (*black dashed line* and *solid line*, respectively)

Results

Mean values (and standard deviations) in the whole group as well as in the subgroups of men and women are reported in Table 1, while Table 2 summarizes the results of repeated measures GLM. SBR values in caudate nucleus and putamen were significantly affected by age ($F_{1,118}$=46.4, p< 0.0001; Fig. 1a, b) and gender ($F_{1,118}$=4.8, p=0.015), while no significant effect was found for handedness and BMI. Moreover, a significant interaction was found between age and region ($F_{3,354}$=8.17, p<0.0001).

The mean SBR value was higher for women than for men (5.62 versus 5.17, standard error 0.27) and decreased with age at a mean rate of 0.0306 per year (0.57 % of the general mean). The slopes of SBR values as a function of age for men and women are shown in Fig. 1a and b for caudate nucleus and putamen, respectively. In these figures, the difference between men and women might visually seem to be higher for the younger ages, but since age-gender interaction was not statistically significant at GLM analysis a common slope was considered in the following as well as for the regression lines. On the other hand, the significant age-region interaction indicated regional differences in age-related decreasing rate, which was 0.028 for left caudate nucleus, 0.026 for right caudate nucleus and 0.034 for both left and right putamen. This different age-related decline for caudate nucleus and putamen was confirmed by the analysis of P/C ratio, showing that age-related SBR decrease was stronger in putamen than in caudate nucleus ($F_{1,120}$=25.31, p<0.0001). The different age-dependent slopes of SBR in caudate nucleus and putamen as a function of age is illustrated in Fig. 2, and the slopes of ratio values are reported in Fig. 3.

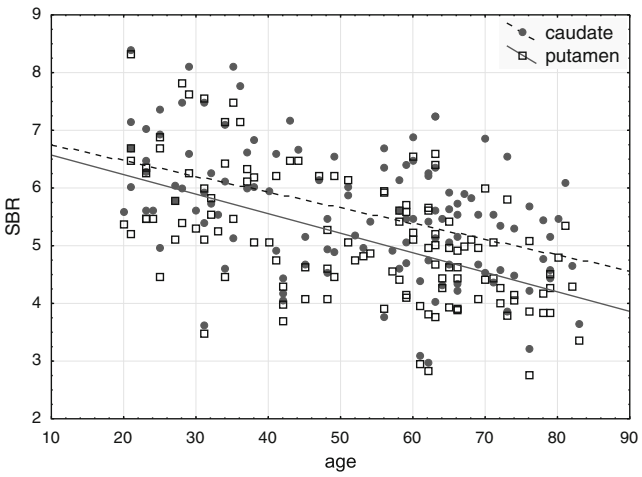

Fig. 2 Scatter plot of SBR as a function of age in the whole group. Data relevant to caudate nucleus (*closed circles*) and putamen (*empty squares*) have been independently fitted by linear regression lines (*black dashed line* and *solid line*, respectively)

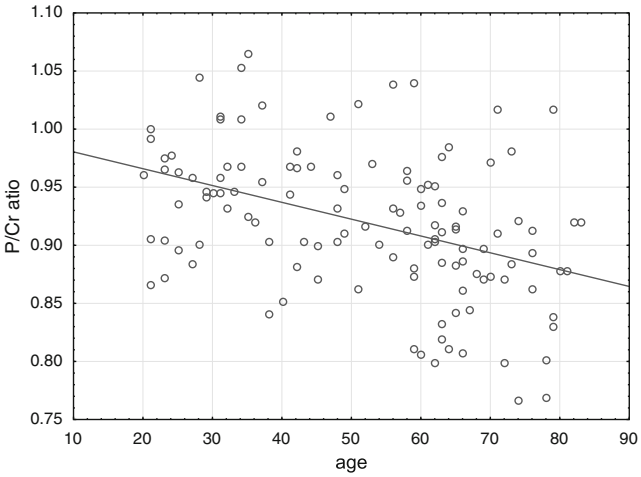

Fig. 3 Scatter plot of the ratio between putamen and caudate nucleus SBR values as a function of age in the whole group of subjects. Data are fitted by a linear regression line

On the other hand, the analysis of per cent asymmetries showed that there was no significant age dependency of inter-hemispheric differences. Absolute values of inter-hemispheric asymmetries (i.e. irrespective of side predominance) were also analysed by repeated measures GLM and a weakly significant effect of age was found ($F_{1,119}$=5.23, p= 0.024) indicating a mild increase of asymmetries with age, without any significant regional difference (see Fig. 4 for the common slope).

The residual of SBR values in caudate nucleus and putamen, after subtraction of age and gender effects, were further analysed to check for the effects of season or time of day when the scan was acquired, but no significant effect was found.

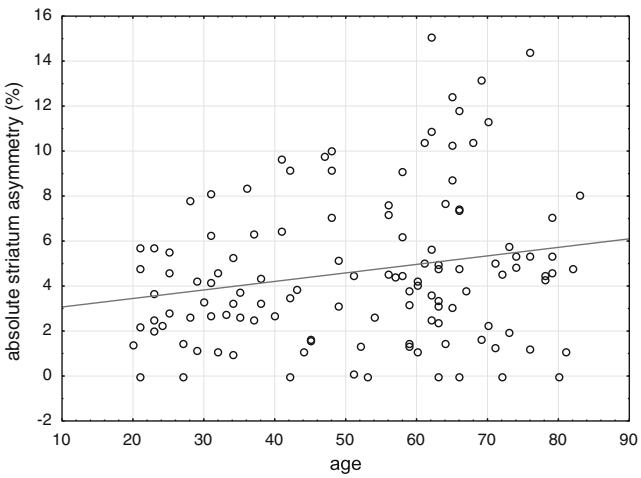

Fig. 4 Scatter plot of the absolute values of the per cent inter-hemispheric asymmetry. Per cent asymmetry was evaluated for both caudate nucleus and putamen, converted into an absolute value and then a mean value was computed for each subject as no significant differences were found between caudate and putamen. These values were then fitted by a linear regression line showing a slight increase with age

According to the effect of age and gender on caudate nucleus and putamen SBR values, and to the age-region interaction, the four equations reported in Table 3 may serve to compute whether a given subject studied in clinical practice has likely normal or abnormal values, provided the above-mentioned acquisition and reconstruction protocols and BasGan V2 software for semi-quantification are used. The width of the prediction intervals around the regression line was not found to vary significantly (from 1.88 at mean age of 50 to 1.91 at extreme ages as for caudate nucleus; from 1.77 at mean age of 50 to 1.79 at extreme ages for putamen). For this reason the more restrictive minimum value (1.88 for caudate nucleus and 1.77 for putamen) was considered for the formulas in Table 3.

Discussion

The main objectives of this study were to examine the effects of age, gender, BMI and other factors on DAT availability, as elaborated by the software BasGan V2 that had been validated in patients with PD or essential tremor and allows 3-D, automatic segmentation of basal ganglia with computation of SBR and PVE [12]. It is free, easy-to-use and produces results in a couple of minutes, without the need of a coregistered MRI. The main limitation is that the shape and dimension of basal ganglia are derived by the Talairach atlas and thus may be inaccurate in extreme cases of very large or very small nuclei or with dysmorphism, which however pertains to a minority of subjects. Also, since the BasGan volumetric regions of interest (VROI) are rigid and do not take into account the possible volume reduction due to atrophy in the elderly population, the effect of ageing may be overestimated. The software is widely used in Europe [11, 19], both for clinical and research purposes [20–25], besides being quoted by the EANM guidelines [26]. VROIs extracted with BasGan express the motor severity of PD better than manual ROI [12], although comparison with other sound automatic methods [5–10] is still lacking.

Table 3 Formulas for the practical estimation of expected SBR values, P/C ratio and absolute asymmetry values with relevant prediction intervals, as functions of age and gender. Prediction intervals are expected to include 95 % of the general population of healthy subjects

Gender	Region	Expected SBR
Men		
	Caudate	$SBR = 6.800 - 0.0273 * age \pm 1.88$
	Putamen	$SBR = 6.702 - 0.0339 * age \pm 1.77$
Women		
	Caudate	$SBR = 7.232 - 0.0273 * age \pm 1.88$
	Putamen	$SBR = 7.116 - 0.0339 * age \pm 1.77$
Index		Expected values
P/C ratio		$\frac{P}{C}ratio = 0.995 - 0.00145 * age \pm 0.113$
Absolute asymmetries		$abs(\%Asymmetry) < 2.688 + 0.0379 * age$

Women showed higher values than men, although this difference tended to disappear with ageing (Fig. 1). This result is in keeping with some previous studies [27–30], whereas other studies failed to find such a difference [31, 32]. The reason for this difference is not clear. A hypothesis might be that women have a higher DAT striatum expression (i.e. higher density), which might be related to higher DA transmission or turnover. Alternatively, gender differences might be related to striatal volume differences [33]. BasGan VROI shape and dimension do not take into account striatal volume and, admitting that men have a slightly larger striatum, this would have caused relatively lower density counts in VROI of women rather than in those of men. In fact, the difference tends to disappear with ageing, while volume of brain structures does not.

The age-related decline of DAT availability measured in this study was 5.7 % per decade, which is in agreement with previous studies reporting values ranging from 4 to 8 %. The other large study of DAT availability and age performed with [^{123}I]β-CIT SPECT reported an average 6.5 % decline of DAT per decade [34], very close to the present data.

Of note, the DAT decline with ageing was more evident at putamen than at caudate level. There are conflicting data in the literature on this topic. By means of [^{18}F]FP-CIT positron emission tomography (PET), a greater age-related decline of DAT was observed at caudate (7.7 % per decade) than at putamen (6.4 % per decade) level, but this finding was observed in a group of only seven normal subjects [35]. Another study [36] examining 15 healthy subjects aged 23–70 by means of [^{11}C]CFT PET also came to a similar conclusion. A greater DAT decline with ageing at the caudate nucleus level was also reported by means of [^{11}C]CFT PET in 16 healthy volunteers [37]. These last authors commented that age-related cell loss in the substantia nigra is likely to preferentially affect its dorsomedial part [38], which projects to the caudate nucleus [39]. They argued that neuronal loss occurs at a rate of 4.7–6.0 % per decade in the substantia nigra [38], approximately the same as the DAT rate decline.

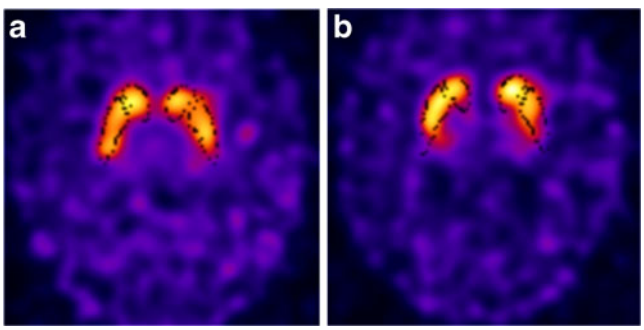

Fig. 5 [^{123}I]FP-CIT SPECT axial section images in two healthy volunteers, aged 23 (**a**) and 83 (**b**). VROI (*black dots*) dimension is fixed. The old subject shows a slightly reduced uptake in the posterior putamen as compared to the young subject

However, these findings in small groups of subjects have not been confirmed by two larger studies in healthy subjects by means of [^{123}I]β-CIT [34] or ^{99m}Tc-NC100697 [40], showing that DAT decline with ageing was comparable between caudate nucleus and putamen. Differences among studies may depend on several factors, including the tracer used to image DAT, the number and the age range of subjects under study, and the modalities of ROI drawing. In the present study, the caudate 3-D ROI also includes the caudate body and tail, not just the head as in previous papers, and the relatively more sparse nigrocaudate endings at body-tail than at head level [41] might have accounted for a milder decline of DAT concentration in the caudate nucleus as a whole, as compared to putamen. In fact, it has been suggested that dopaminergic neurons projecting to the caudate head have a higher activity than those projecting to the tail and that dopaminergic neurons projecting to the caudate nucleus show topographical differences in their firing rate [42]. Lastly, the greater reduction of putamen uptake with ageing is unlikely to be an artefact of BasGan VROI positioning, as VROI dimension is fixed and thus independent of subject age (examples in Fig. 5).

No correlation was found between DAT uptake and BMI, which had been reported by some authors [43] but then not further confirmed. Recent imaging studies suggested that season may affect serotonin transporter expression [44, 45] and also ^{18}F-dopa uptake in healthy controls [46]. The presently observed absence of significant influence of season and time of day upon DAT levels does not support the hypothesis of seasonal and circadian rhythms in DAT regulation and is moreover reassuring when scans are performed. The lack of circadian variation is in keeping with animal studies suggesting a circadian rhythm of DAT in the nucleus accumbens, but not in the caudate nucleus [47]. Finally, the lack of effect of handedness on DAT should be taken with caution since the number of partial (n=4) or full (n=6) left-handers was rather small and this unbalance with respect to right-handers might have affected the results. An ad hoc investigation with balanced numbers is required to fully elucidate this issue.

Conclusion

A large database of [^{123}I]FP-CIT SPECT scans of healthy controls has been generated and analysed by means of an automatic, easy-to-use software. The analysis of the data have confirmed previous findings of higher DAT availability in women versus men and an age-related DAT decline of 5.7 % per decade. These SPECT data can be used as reference data for nuclear medicine departments performing DaTSCAN® imaging and using BasGan V2 software. The SBR values, ratios and asymmetries reported here can be used as reference only if the same acquisition and reconstruction protocols are used. The use of other reconstruction algorithms (such as the filtered back-projection) or non-attenuation-corrected images may produce different results. Moreover, the use of the present equations and limits obtained with the BasGan software presupposes that the gamma camera is calibrated with a basal ganglia phantom, which can be achieved autonomously or with the support of the EANM. In case such calibration values are unavailable, the phantom-derived calibration ENC-DAT values obtained in the most commonly used gamma camera systems [16] could be used. However, using either calibrated or uncalibrated data allowed similar results in the whole of ENC-DAT subjects [48].

Acknowledgments The participating centres thank GE Healthcare and the German Parkinson Association for their financial contribution to this study, ABX-CRO for managing the network activities and the Executive Committee of the EANM for establishing the EANM Research Ltd. (EARL) as an administrative framework for this project. The authors also thank the personnel from each Nuclear Medicine Centre responsible for the quality controls and acquisition of the SPECT data.

Conflicts of interest Prof. Jan Booij is a consultant for GE Healthcare.

References

1. Benamer TS, Patterson J, Grosset DG, Booij J, de Bruin K, van Royen E, et al. Accurate differentiation of parkinsonism and essential tremor using visual assessment of [123I]-FP-CIT SPECT imaging: the [123I]-FP-CIT study group. Mov Disord 2000;15:503–10.
2. O'Brien JT, Colloby S, Fenwick J, Williams ED, Firbank M, Burn D, et al. Dopamine transporter loss visualized with FP-CIT SPECT in the differential diagnosis of dementia with Lewy bodies. Arch Neurol 2004;61:919–25.
3. Chouker M, Tatsch K, Linke R, Pogarell O, Hahn K, Schwarz J. Striatal dopamine transporter binding in early to moderate advanced Parkinson's disease: monitoring of disease progression over 2 years. Nucl Med Commun 2001;22:721–5.
4. Parkinson Study Group. Dopamine transporter brain imaging to assess the effects of pramipexole vs levodopa on Parkinson disease progression. JAMA 2002;287:1653–61.
5. Acton PD, Pilowsky LS, Kung HF, Ell PJ. Automatic segmentation of dynamic neuroreceptor single-photon emission tomography images using fuzzy clustering. Eur J Nucl Med 1999;26:581–90.
6. Acton PD, Mozley PD, Kung HF. Logistic discriminant parametric mapping: a novel method for the pixel-based differential diagnosis of Parkinson's disease. Eur J Nucl Med 1999;26:1413–23.
7. Koole M, Laere KV, de Walle RV, Vandenberghe S, Bouwens L, Lemahieu I, et al. MRI guided segmentation and quantification of SPECT images of the basal ganglia: a phantom study. Comput Med Imaging Graph 2001;25:165–72.
8. Habraken JBA, Booij J, Slomka P, Sokole EB, van Royen EA. Quantification and visualization of defects of the functional dopaminergic system using an automatic algorithm. J Nucl Med 1999;40:1091–7.
9. Radau PE, Linke R, Slomka PJ, Tatsch K. Optimization of automated quantification of 123I-IBZM uptake in the striatum applied to parkinsonism. J Nucl Med 2000;41:220–7.
10. Koch W, Radau PE, Hamann C, Tatsch K. Clinical testing of an optimized software solution for an automated, observer-independent evaluation of dopamine transporter SPECT studies. J Nucl Med 2005;46:1109–18.
11. Tatsch K, Poepperl G. Quantitative approaches to dopaminergic brain imaging. Q J Nucl Med Mol Imaging 2012;56:27–38.
12. Calvini P, Rodriguez G, Inguglia F, Mignone A, Guerra UP, Nobili F. The basal ganglia matching tools package for striatal uptake

semi-quantification: description and validation. Eur J Nucl Med Mol Imaging 2007;34:1240–53.
13. Derogatis LR, Unger R. Symptom checklist-90-revised. The Corsini encyclopedia of psychology. Hoboken: Wiley; 2010. p. 1–2.
14. Beck AT, Ward CH, Mendelson M, Mock J, Erbaugh J. An inventory for measuring depression. Arch Gen Psychiatry 1961;4:561–71.
15. Fazekas F, Niederhorn K, Schmidt R, Offenbacher H, Horner S, Bertha G, et al. White matter signal abnormalities in normal individuals: correlation with carotid ultrasonography, cerebral blood flow measurements, and cerebrovascular risk factors. Stroke 1988;19:1285–8.
16. Tossici-Bolt L, Dickson JC, Sera T, de Nijs R, Bagnara MC, Jonsson C, et al. Calibration of gamma camera systems for a multicentre European 123I-FP-CIT SPECT normal database. Eur J Nucl Med Mol Imaging 2011;38:1529–40.
17. Dickson JC, Tossici-Bolt L, Sera T, de Nijs R, Booij J, Bagnara MC, et al. Proposal for the standardisation of multi-centre trials in nuclear medicine imaging: prerequisites for a European 123I-FP-CIT SPECT database. Eur J Nucl Med Mol Imaging 2012;39:188–97.
18. Electronic Statistics Textbook. (Electronic Version): StatSoft, Inc. (2011). Tulsa, OK: StatSoft. WEB: http://www.statsoft.com/textbook/.(Printed Version): Hill, T. & Lewicki, P. (2007). STATISTICS: Methods and Applications. StatSoft, Tulsa, OK.
19. Badiavas K, Molyvda E, Iakovou I, Tsolaki M, Psarrakos K, Karatzas N. SPECT imaging evaluation in movement disorders: far beyond visual assessment. Eur J Nucl Med Mol Imaging 2011;38:764–73.
20. Pagan L, Tranfaglia C, Galli S, Lucchi G, Novi B, Fagioli G, et al. A comparison between the conventional manual ROI method and an automatic algorithm for semi quantitative analysis of SPECT studies. International Conference on Image Optimisation in Nuclear Medicine (OptiNM) J Phys: Conference Series 317 (2011) 012004.
21. Isaias IU, Marotta G, Pezzoli G, Sabri O, Schwarz J, Crenna P, et al. Enhanced catecholamine transporter binding in the locus coeruleus of patients with early Parkinson disease. BMC Neurol 2011;11:88.
22. Caobelli F, Paghera B, Giubbini R. Is the time ripe to adopt semi-quantitative analysis of SPECT evaluation in movement disorders as a standard? Eur J Nucl Med Mol Imaging 2011;38:596–7.
23. Nobili F, Campus C, Arnaldi D, De Carli F, Cabassi G, Brugnolo A, et al. Cognitive-nigrostriatal relationships in de novo, drug-naïve Parkinson's disease patients: a [I-123]FP-CIT SPECT study. Mov Disord 2010;25:35–43.
24. Nobili F, Arnaldi D, Campus C, Ferrara M, De Carli F, Brugnolo A, et al. Brain perfusion correlates of cognitive and nigrostriatal functions in de novo Parkinson's disease. Eur J Nucl Med Mol Imaging 2011;38:2209–18.
25. Arnaldi D, Campus C, Ferrara M, Famà F, Picco A, De Carli F, et al. What predicts cognitive decline in de novo Parkinson's disease? Neurobiol Aging 2012;33:1127.e11–20.
26. Darcourt J, Booij J, Tatsch K, Varrone A, Vander Borght T, Kapucu OL, et al. EANM procedure guidelines for brain neurotransmission SPECT using (123)I-labelled dopamine transporter ligands, version 2. Eur J Nucl Med Mol Imaging 2010;37:443–50.
27. Lavalaye J, Booij J, Reneman L, Habraken JBA, van Royen EA. Effect of age and gender on dopamine transporter imaging with [123I]FP-CIT SPECT in healthy volunteers. Eur J Nucl Med 2000;27:867–9.
28. de Rijk MC, Launer LJ, Berger K, Breteler MM, Dartigues JF, Baldereschi M, et al. Prevalence of Parkinson's disease in Europe: a collaborative study of population-based cohorts. Neurologic Diseases in the Elderly Research Group. Neurology 2000;54(11 Suppl 5):S21–3.
29. Staley JK, Krishnan-Sarin S, Zoghbi S, Tamagnan G, Fujita M, Seibyl JP, et al. Sex differences in [123I]beta-CIT SPECT measures of dopamine and serotonin transporter availability in healthy smokers and nonsmokers. Synapse 2001;41:275–84.
30. Mozley LH, Gur RC, Mozley PD, Gur RE. Striatal dopamine transporters and cognitive functioning in healthy men and women. Am J Psychiatry 2001;158:1492–9.
31. de Rijk MC, Tzourio C, Breteler MM, Dartigues JF, Amaducci L, Lopez-Pousa S, et al. Prevalence of parkinsonism and Parkinson's disease in Europe: the EUROPARKINSON Collaborative Study. European Community Concerted Action on the Epidemiology of Parkinson's disease. J Neurol Neurosurg Psychiatry 1997;62:10–5.
32. Ryding E, Lindström M, Brådvik B, Grabowski M, Bosson P, Träskman-Bendz L, et al. A new model for separation between brain dopamine and serotonin transporters in 123I-beta-CIT SPECT measurements: normal values and sex and age dependence. Eur J Nucl Med Mol Imaging 2004;31:1114–8.
33. Gunning-Dixon FM, Head D, McQuain J, Acker JD, Raz N. Differential aging of the human striatum: a prospective MR imaging study. AJNR Am J Neuroradiol 1998;19:1501–7.
34. van Dyck CH, Seibyl JP, Malison RT, Laruelle M, Zoghbi SS, Baldwin RM, et al. Age-related decline in dopamine transporters: analysis of striatal subregions, nonlinear effects, and hemispheric asymmetries. Am J Geriatr Psychiatry 2002;10:36–43.
35. Kazumata K, Dhawan V, Chaly T, Antonini A, Margouleff C, Belakhlef A, et al. Dopamine transporter imaging with fluorine-18-FPCIT and PET. J Nucl Med 1998;39:1521–30.
36. Rinne JO, Sahlberg N, Ruottinen H, Någren K, Lehikoinen P. Striatal uptake of the dopamine reuptake ligand [11C]beta-CFT is reduced in Alzheimer's disease assessed by positron emission tomography. Neurology 1998;50:152–6.
37. Ishibashi K, Ishii K, Oda K, Kawasaki K, Mizusawa H, Ishiwata K. Regional analysis of age-related decline in dopamine transporters and dopamine D2-like receptors in human striatum. Synapse 2009;63:282–90.
38. Gibb WR, Lees AJ. Anatomy, pigmentation, ventral and dorsal subpopulations of the substantia nigra, and differential cell death in Parkinson's disease. J Neurol Neurosurg Psychiatry 1991;54:388–96.
39. Szabo J. Organization of the ascending striatal afferents in monkeys. J Comp Neurol 1980;189:307–21.
40. Koch W, Pogarell O, Pöpperl G, Hornung J, Hamann C, Gildehaus FJ, et al. Extended studies of the striatal uptake of 99mTc-NC100697 in healthy volunteers. J Nucl Med 2007;48:27–34.
41. Carpenter MB, Peter P. Nigrostriatal and nigrothalamic fibers in the rhesus monkey. J Comp Neurol 1972;144:93–116.
42. Nomoto M, Kaseda S, Iwata S, Shimizu T, Fukuda T, Nakagawa S. The metabolic rate and vulnerability of dopaminergic neurons, and adenosine dynamics in the cerebral cortex, nucleus accumbens, caudate nucleus, and putamen of the common marmoset. J Neurol 2000;247 Suppl 5:V16–22.
43. Chen PS, Yang YK, Yeh TL, Lee I-H, Yao WJ, Chiu NT, et al. Correlation between body mass index and striatal dopamine transporter availability in healthy volunteers—a SPECT study. Neuroimage 2008;40:275–9.
44. Ruhé HG, Booij J, Reitsma JB, Schene AH. Serotonin transporter binding with [123I]beta-CIT SPECT in major depressive disorder versus controls: effect of season and gender. Eur J Nucl Med Mol Imaging 2009;36:841–9.
45. Kalbitzer J, Erritzoe D, Holst KK, Nielsen FA, Marner L, Lehel S, et al. Seasonal changes in brain serotonin transporter binding in short serotonin transporter linked polymorphic region-allele carriers but not in long-allele homozygotes. Biol Psychiatry 2010;67:1033–9.
46. Eisenberg DP, Kohn PD, Baller EB, Bronstein JA, Masdeu JC, Berman KF. Seasonal effects on human striatal presynaptic dopamine synthesis. J Neurosci 2010;30:14691–4.
47. Sleipness EP, Sorg BA, Jansen HT. Diurnal differences in dopamine transporter and tyrosine hydroxylase levels in rat brain: dependence on the suprachiasmatic nucleus. Brain Res 2007;1129:34–42.
48. Varrone A, Dickson J, Tossici-Bolt L, Sera T, Asenbaum S, Booij J, et al. European multicentre database of healthy controls for [(123)I]FP-CIT SPECT (ENC-DAT): age-related effects, gender differences and evaluation of different methods of 3 analysis. Eur J Nucl Med Mol Imaging. doi:10.1007/s00259-012-2276-8.